ESTIMATING FLOW CONCENTRATION AND SEDIMENT REDISTRIBUTION ON SALINE RANGELAND COMMUNITIES

Sayjro K Nouwakpo, Research Professor, University of Nevada Reno, Department of Natural Resources and Environmental Science, snouwakpo@cabnr.unr.edu 775-784-6056; Mark Weltz, Rangeland Hydrologist and Research Leader, United States Department of Agriculture, Agriculture Research Service, mark.weltz@ars.usda.gov, 775-784-6057; Kenneth McGwire Associate Research Professor, Desert Research Institute, Division of Earth and Ecosystem Sciences, Ken.McGwire@dri.edu, 775-673-7324; Colleen G. Rossi, Water Quality Salinity Specialist, Bureau of Land Management, Salt Lake City, Utah, crossi@blm.gov, (801) 539-4028

ABSTRACT

In arid and semi-arid rangelands where vegetation is typically sparse, a synergistic relationship is assumed to exist between spatial distribution of plants and hydrologic and erosion processes. In these environments, an accurate understanding of sediment transport processes is key to developing informed management actions and addressing ecosystem response to global changes. In this study, data from rainfall simulation experiments in saline rangeland communities of the Upper Colorado River Basin were used to improve understanding on various sediment and solute transport processes in field conditions. During these experiments, hydrology, erosion and high-resolution surface microtopography changes were routinely measured, presenting a unique opportunity to answer many sediment transport questions relevant to these saline rangeland and other sparsely vegetated ecosystems. A series of variables were developed to quantify and characterize surface microtopographic changes as a function of hydrology, erodibility and hillslope configuration. Key findings from preliminary analyses include: (1) the dependence of deposition on plot slope and its independence on hydrologic and soil loss variables, (2) data supporting the process of increased downcutting as slope increased, (3) significance of accounting deposition processes in overall runoff energy quantification, (4) evidence of an equilibrium channel geometry with a given discharge that is marginally impacted by runoff duration.

INTRODUCTION

Hillslope runoff and soil erosion processes play a vital role in rangeland ecosystem sustainability due to their control on resource mobility but they also have significant implications in off-site resource transport. Nichols et al. (2013) found for example that hillslope processes contributed to 85% of sediment delivery from a 43.7 ha semi-arid shrub-dominated watershed. The influence of vegetation on hillslope runoff and sediment production forms the basis of current hydrology and erosion modeling technologies on rangelands (Nearing et al., 2011). Early attempts to apply empirical soil erosion models derived primarily from cropland data, such as the Universal Soil Loss Equation – USLE and the Revisited Universal Soil Loss Equation – RUSLE, on rangelands yielded unsatisfactory and contested results (Blackburn, 1980; Foster et al., 1981; Hart, 1984; Johnson et al., 1984; Mitchell and Roundtable, 2010; Spaeth et al., 2003; Trieste and Gifford, 1980). Weltz et al. (1998) point to the lumped nature and rigid structure of these empirical models as a key deficiency when applied to rangelands where biotic and abiotic interactions play a strong control on surficial processes.

The advent of physically-based soil erosion models such as the Water Erosion Prediction Project model-WEPP (Laflen et al., 1991) offered the opportunity to develop the scientific framework necessary to provide insight into the relationship between hydrologic processes and rangeland condition. These research efforts led to the Rangeland Hydrology and Erosion Model (RHEM) (Nearing et al., 2011), developed from experimental data specifically collected on rangeland sites across the Western U.S. As a process-based erosion model, RHEM models erosion and hydrology using the same fundamental principles as WEPP.

Runoff generation and erosion on the hillslope are modeled in response to hydrological inputs and hydraulic parameters that are adjusted based on soil intrinsic properties and land surface conditions.

In both WEPP and RHEM, the hillslope is divided into interrill areas where splash and sheet detachment and transport occur and rills where flow is concentrated and fluvial processes dominate. Accurate partitioning of hillslope erosion into interrill and concentrated-flow-dominated processes has a significant implication on rangeland erosion modelling especially following disturbances. Several studies (e.g, Al-Hamdan et al., 2012; Pierson et al., 2013) have demonstrated a significant increase in concentrated flow erosion when shrub-dominated rangeland are disturbed by fire or woody species encroachment compared to undisturbed conditions.

Concentrated flow erosion is a complex process because rill networks have a dual function of sediment and runoff production and storage as well as that of transport of these resources off-site and these intricately coupled functions are traditionally assumed to be controlled by rill flow hydraulics. The key to accurate concentrated flow erosion has therefore been that of adequate prediction of hydraulic parameters. A great deal of research efforts have been invested into relating rill detachment rate to flow hydraulic parameters such as average shear stress (e.g., Ghebreiyessus et al., 1994; Lyle and Smerdon, 1965; Nearing et al., 1997; Torri et al., 1987), stream power (e.g., Bagnold, 1977; Nearing et al., 1997; Zhang et al., 2003), effective stream power (e.g., Bagnold, 1980). Performance tests of these hydraulic parameters at predicting rill detachment rate in various experimental conditions (Al-Hamdan et al., 2012; Wirtz et al., 2013) resulted in no single parameter consistently best-fitting observed detachment rates, although (Al-Hamdan et al., 2012) found that the stream power performed well with rangeland erosion data. Wirtz et al. (2013) attributed discrepancies between observed and predicted erosions to the inherent emphasis of most hydraulic parameters on fluvial processes incising channel bottoms while diffusive processes such as headcut-retreat and bank-erosion make up a non-negligible portion of rill detachment.

Currently available hydraulic-driven-rill-detachment equations albeit incomplete, offer a widely accepted modeling framework but often rely on a good characterization of the channel network. One of the knowledge gap in process-based soil erosion modeling especially on rangelands is the lack of an adequate framework to characterize spatial extent of concentrated flow network. Another knowledge gap in these process-based modeling approaches concerns the mechanism of deposition.

As part of an effort to quantify salt transport from rangelands to the Upper Colorado River Basin (UCRB), experimental rainfall simulation studies were conducted in saline rangelands communities of this basin. Hydrology, erosion and high-resolution surface microtopography changes were routinely measured during these simulations, presenting a unique opportunity to answer many sediment transport questions relevant to these saline rangelands and other sparsely vegetated rangelands. The aim of this paper was to gain insight into the processes of concentrated flow erosion and deposition on saline rangelands by relating traditionally measured hydrologic and sediment yield data to observed expression of these processes in surface microtopography. This knowledge would provide a predictive framework for hydraulic parameter estimation on saline rangelands for use in physically-based erosion models such as RHEM.

MATERIAL AND METHODS

Study area: This study was part of a broader research effort aimed at quantifying salt transport from rangelands to the Upper Colorado River headwaters. Previous researchers (e.g., Hawkins et al., 1977; Riley et al., 1979; Tuttle and Grauch, 2009) have identified upland areas of the Upper Colorado River Basin in the Mancos Shale and Eagle Valley Evaporite geologic formations as major contributor to the river's salinity. For our study, two sites (Price and DryX hereafter) in the Mancos Shale geologic formation were then selected to conduct rainfall simulation experiments. These sites were selected for their contrasting slope ranges and differences in intrinsic properties of the soil.

The Price site was located near the city of Price, Utah at the geographic coordinates 39° 27' 47.22"N 110° 36' 26.16"W and average elevation of 1649 m. The soil on this site was mapped as a Persayo loam soil series and classified as loamy, mixed, active, calcareous, mesic, shallow, typic torriorthents. Measured slopes on the experimental site ranged from 0.6 to 10%. DryX was located near the city of Ferron, Utah at the geographic coordinates 38°58'38.50"N 111° 7'10.60"W and average elevation of 1893 m. The predominant soil type at DryX was mapped as a complex of Chipeta series soils with Badland areas. The taxonomic classification of the Chipeta series is clayey, mixed, active, calcareous, mesic, shallow, typic torriorthents. Measured slopes at the study area of the DryX site ranged from 11.4% to 24.5%.

Experimental setup

On each experimental site, a series of rainfall simulations were conducted on 6 m x 2 m erosion plots to quantify sediment and salt transport processes during rainfall-driven erosion processes. Erosion and hydrologic responses were assessed by measuring soil loss, runoff and solute transport under four rainfall intensities corresponding to return periods of 2 (50.8 mm/hr), 10 (88.9 mm/hr), 25 (114.3 mm/hr) and 50 (139.7 mm/hr) years. On each plot, a single rainfall event was applied to ensure the capture of the process of salt efflorescence (Bowles et al., 1982; Riley et al., 1982) whereby a salt crust is left at the soil surface by evaporation. Each rainfall intensity on each site was replicated three times leading to a total of twelve plots per site.

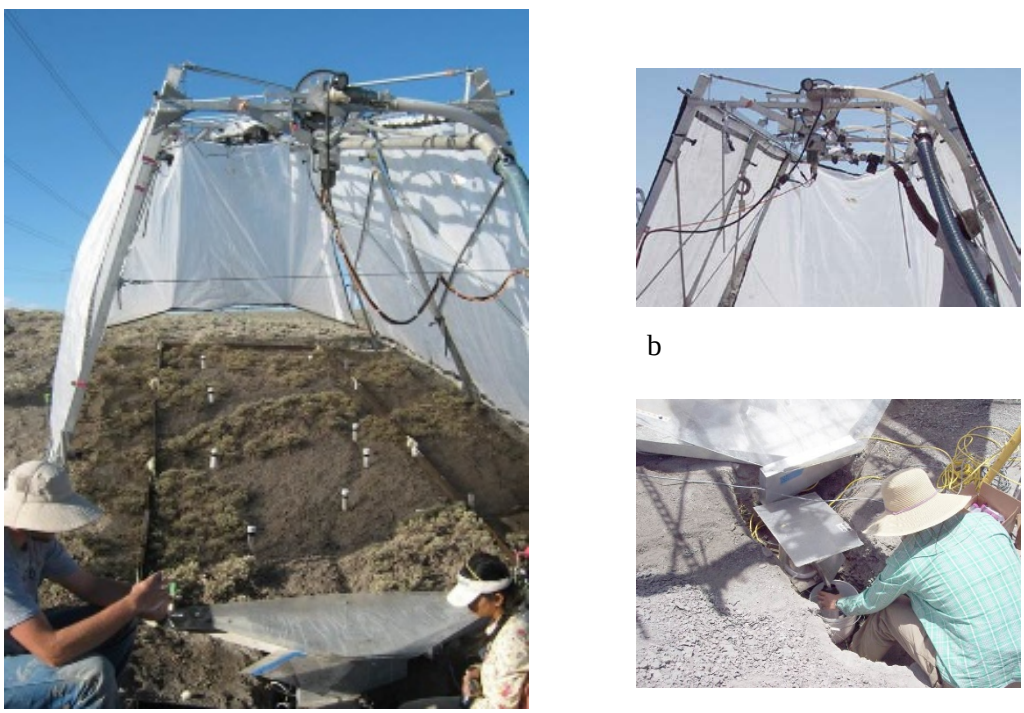

a b c

Figure 1 Experimental setup showing (a) rainfall simulator on 6 m x 2 m plot, (b) a close-up view of the camera mount and rail mechanism and (c) the supercritical flume used for runoff discharge measurement and runoff sampling.

A Walnut Gulch Rainfall Simulator (WGRS) (Paige et al., 2004) was used in this study (Figure 1a). A rail mechanism mounted lengthwise on the frame of the simulator supported a camera (Figure 1b) which was used to take overlapping pictures before and after each rainfall event to reconstruct soil surface microtopography at sub-millimeter resolution. A digital Single Lens Reflex (SLR) camera equipped with a

20 mm lens was used for acquiring the surface reconstruction pictures. The average camera-ground distance was 2.4 m and the overlap between adjacent pictures 0.15 m. Pictures were taken along two paths 0.76 m apart on either side of the central boom of the simulator. This image network configuration resulted in 80 to 90 pictures to cover each plot. Translucent side curtains on the simulator served the dual purpose of diffusing light, reducing excessive shadowing in the pictures and limited the effect of wind on rainfall distribution.

Soil surface analysis: Soil surface microtopography was reconstructed using the structure from motion software Agisoft PhotoScan 1.0 (Agisoft Llc, 2013). For each plot, PhotoScan produced pre- and post-rain point clouds which were manually edited to remove vegetation points in the software Cloud Compare (General Public Licence, 2014). Vegetation-free point clouds were then converted in Digital Elevation Models (DEMs) (Figure 2) and analyzed within the ArcGIS system (Esri, 2011).

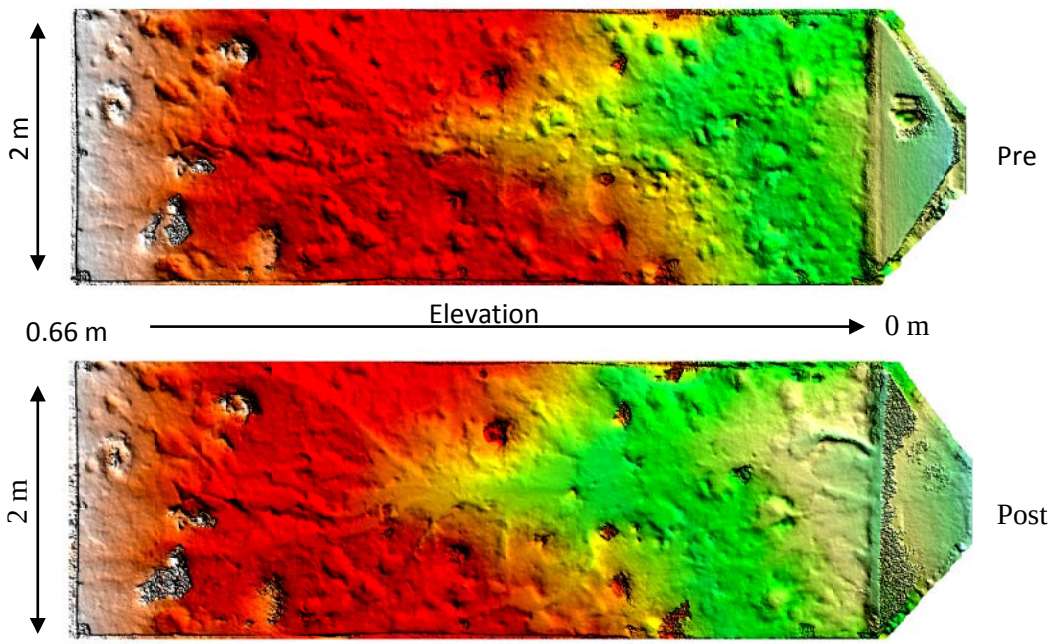

Figure 2 Example of 5-mm resolution DEMs representing soil microtopography reconstructed pre and post rainfall.

In this paper, changes in soil surface microtopography were related to sediment transport mechanisms. Changes to soil surface microtopography were quantified by subtracting post- from pre-rain DEMs, allowing the distinction between erosion areas (negative difference) and deposition areas (positive difference). To characterize soil surface response to erosive events, various areal and volumetric surface metrics were calculated from pre- and post-rain DEMs as well as the difference of DEMs.

Total erosion, deposition and net loss: The overall spatial extents of erosion processes TX_E and deposition TX_D were calculated as

$$TX_E = n \times A \tag{1}$$

$$TX_D = m \times A \tag{2}$$

where n and m are the number of grid cells with respectively negative and positive DEM differences and A is the grid size.

The volumes TV_E, TV_D and TV_N corresponding to erosion and deposition and net loss processes were also quantified as

$$TV_E = \sum_{i=0}^{i=n} \Delta Z_i \times A \tag{3}$$

$$TV_D = \sum_{j=0}^{j=m} \Delta Z_j \times A \tag{4}$$

$$TV_N = TV_E - TV_D \tag{5}$$

where *i* and *j* are respectively grid positions of erosion and deposition and ΔZ is the magnitude of elevation change.

Channel processes: Understanding mechanisms of erosion processes in concentrated flow pathways as they relate to other landscape attributes is crucial to accurate soil erosion modeling. In this study, flow concentration pathways were identified by applying the bottom-hat (also known as the black top-hat) mathematical morphology to the original DEMs. The bottom-hat operator detects local extrema in a two dimensional signals such as images and DEMs. This operator has been successfully applied to digital topographic data to delineate flow network and detect erosional incision (e.g., Rodriguez et al., 2002; Schwanghart et al., 2013). The detail presentation of the bottom-hat implementation is beyond the scope of this paper but in our study, the output of this operator was a spatial function whose minima were areas in the DEMs of local concavities. To minimize the effect of surface roughness in channel network detection, the original DEMs were smoothed using a 0.125 m^2 diamond-shaped structuring element similar to that used in Hyun-Chong et al. (2006). Concentrated flow pathways were considered as areas with bottom-hat responses lower than the plot average. Flow networks corresponding to the conditions pre- (Net_{pre}) and post- (Net_{post}) rain were merged to give a final flow network *Net*.

Spatial extent of erosion and deposition (CX_E and CX_D) that occurred within channels were obtained in a similar manner as TX_E and TX_D.

$$CX_E = n_c \times A \tag{6}$$

$$CX_D = m_c \times A \tag{7}$$

where n_c and m_c are the number of grid cells with respectively negative and positive DEM differences within *Net*. Likewise, CV_E, CV_D and CV_N were calculated by applying Eq. 3-5 to areas within *Net*.

Erosive forces can alter channel networks in both vertical and lateral dimensions depending on hillslope characteristics. These directional changes to the channel network were captured in $Net_{\Delta xy}$ and $Net_{\Delta z}$ for lateral and vertical changes respectively as:

$$Net_{\Delta xy} = Net_{post} \backslash Net_{pre} \tag{8}$$

$$Net_{\Delta z} = Net_{post} \cap Net_{pre} \tag{9}$$

where \ is the set difference operator and ∩ the intersection operator.

From the $Net_{\Delta xy}$ sub-network, spatial and volumetric metrics CX_{xyE}, CX_{xyD}, CV_{xyE}, CV_{xyD} and CV_{xyN} were calculated whereas $Net_{\Delta z}$ was used to obtain CX_{zE}, CX_{zD}, CV_{zE}, CV_{zD} and CV_{zN}.

Other secondary parameters were also calculated:

$$CXR = (CX_E + CX_D)/(TX_E + TX_D) \tag{10}$$

$$CVR_E = CV_E/TV_E \tag{11}$$

$$CVR_N = CV_N/TV_N \tag{12}$$

CXR, CVR_E and CVR_D express the space-based and volume-based ratio of concentrated flow processes that occurred on a plot.

The proportion of concentrated flow energy expenditure in lateral channel expansion versus vertical growth was quantified using two parameters α and α' calculated as:

$$\alpha = CV_{xyE}/CV_E \tag{13}$$

$$\alpha' = CV_{xyN}/CV_N \tag{14}$$

Deposition processes were also examined by calculating the proportion of eroded volume that was re-deposited at the plot level (*TDR*) and in the channels (*CDR*).

$$TDR = TV_D/TV_E \tag{15}$$

$$CDR = CV_D/CV_E \tag{16}$$

These surface changes metrics were related to hydrologic and erosion variables as well as plot slope (SLP). Hydrologic variables used were precipitation (*P*), runoff discharge (*R*), infiltration rate (*IR*), cumulative runoff (SR) and erosion information were sediment concentration (SC) and total sediment loss (S). Throughout this paper, the units are m^2 for spatial metrics (e.g., TX_E, CX_E), m^3 for volumetric surface metrics (e.g., TV_E, CV_E). *P*, *R* and *IR* are in mm, *SR* in 10^{-3} m^3, *SC* in g/L and *S* is in g.

PRELIMINARY RESULTS FROM THE PRICE SITE

Plot-wide erosion and deposition processes: Figure 3 shows the relationships between calculated plot-wide-surface-change metrics and hydrology, erosion and plot slope gradient. For erosion processes, volumetric metrics improved the correlation with hydrology and erosion variables (increased R^2) compared to the spatial metrics (e.g., TX_E vs TV_E), suggesting that incorporating the depth information is crucial to understanding erosion and deposition processes. This improvement in R^2 with the incorporation of depth information was observed throughout the analyses in this study therefore area-based metrics have been excluded as much as possible from other figures for conciseness.

TV_E had the highest correlation in all comparisons except with slope with which TX_E performed better, suggesting that in our experimental conditions at Price, overall eroded volumes were not a function of slope. Cumulative runoff *SR* and runoff rate *R* were better predictors of erosion volumes TV_E with R^2 of 0.60 and 0.74 compared to sediment concentration *SC* and cumulative sediment *S* (R^2 = 0.14 and 0.38 respectively). This finding suggests that a portion of observed sediment loss by weight (especially the colloidal soil fraction) has little contribution to overall surface microtopography. Also, runoff rate R better predicted erosion volumes than cumulative runoff. This finding is consistent with the existence of an equilibrium-channel-network-geometry for a specific runoff discharge with marginal influence of runoff duration. It is also important to note that rainfall events at the Price site did not vary significantly in length which may have masked the effect of runoff duration.

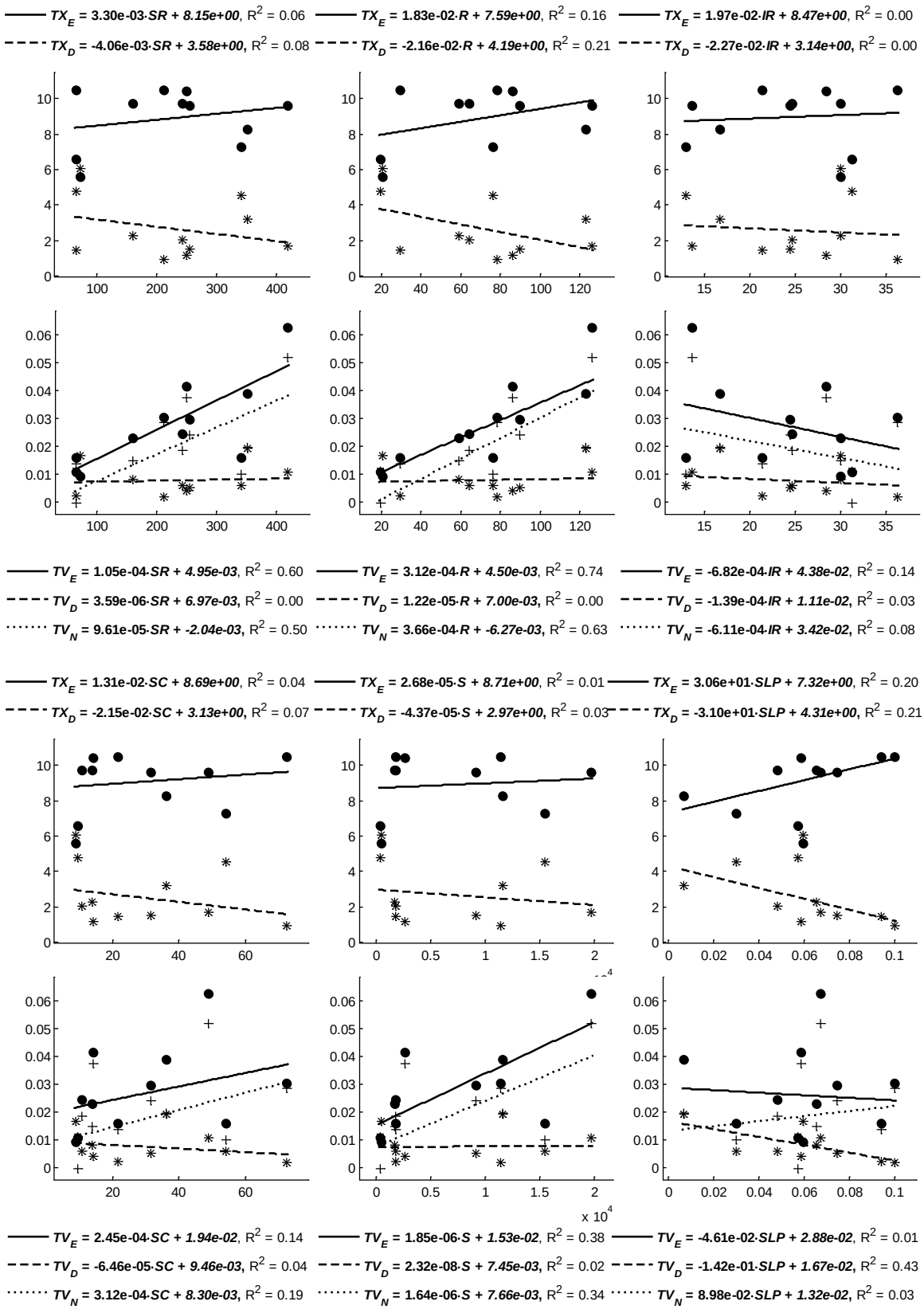

Figure 3 Plot-wide surface change metrics as a function of hydrology, erosion and slope variables.

Deposition processes (TX_D and TV_D) performed poorly against all hydrologic and erosion processes. For hydrologic processes, the largest correlation was found between TX_D and R with an R^2 of 0.21 but it is important to note that TX_D and TX_E are strongly correlated since they are complement of one another on a fixed plot area. This lack of dependence of deposition processes on hydrologic and erosion processes was likely the cause of the decrease in R^2 observed in most cases (except TV_E, TV_N vs. SC) when TV_E was replaced with TV_N. Nevertheless TV_D showed a systematic decreasing trend with slope (R^2 = 0.43), suggesting that sediment deposition volume was mainly controlled by plot slope on this site.

Channel processes: Figure 4 summarizes results of the microtopographic analysis in concentrated flow areas.

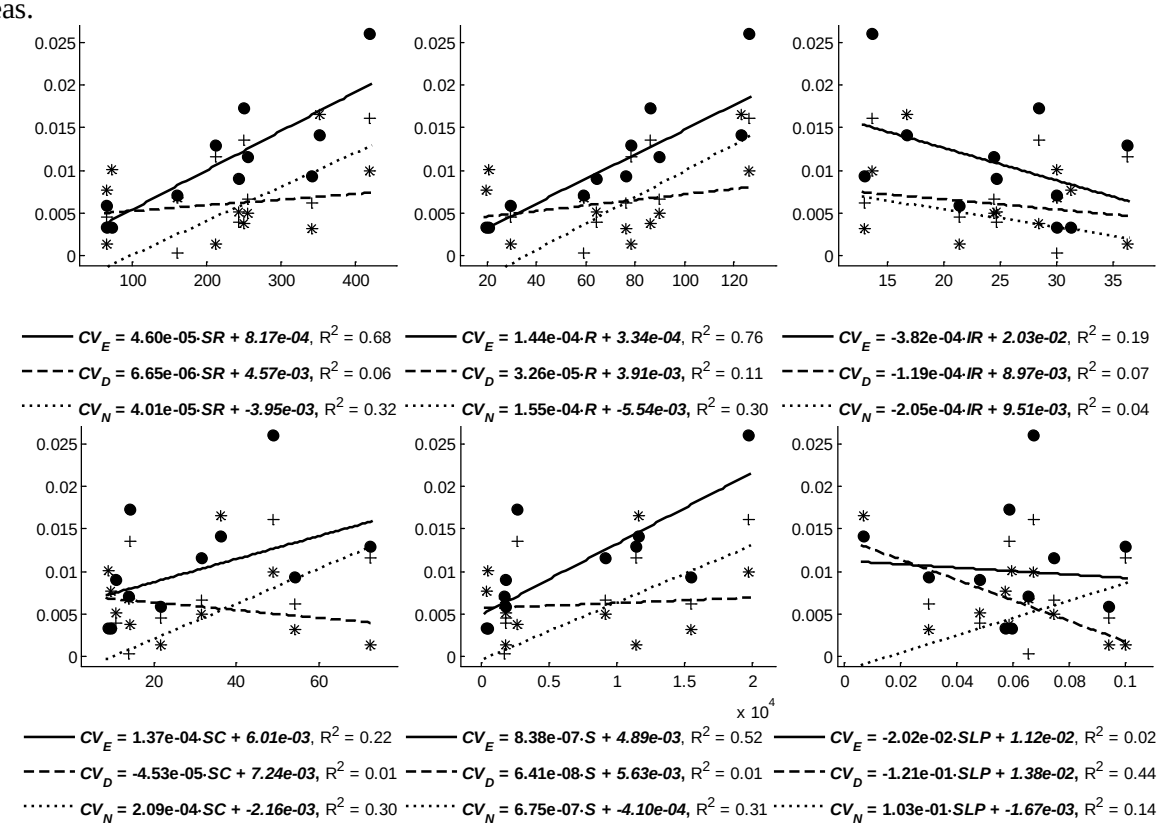

Figure 4 Concentrated flow processes as a function of hydrology, erosion and slope

Overall observations made for the plot-wide analysis are also valid here: (1) the incorporation of depth information in erosion volumes in channels improved correlation correlated with all variables (here again except for slope) with R^2 values for CV_E larger than those of CX_E (not shown in Figure 4), (2) runoff rate was a better predictor of eroded volume than cumulative runoff, (3) hydrology variables were better predictors of eroded volumes in channels than observed soil loss, (4) within channel deposition was primarily controlled by slope. Surface change metrics measured in channels were better correlated with hydrology, soil loss and slope variables than were plot-wide metrics indicated by an increase in R^2 in 21 of the 30 linear regressions on Figure 3 compared to Figure 4. However when TV_E and CV_E are plotted against precipitation P (Figure 5), one notices a slightly stronger correlation of P with TV_E. In other words, when relating surface change metrics to precipitation, R^2 increased with the inclusion of diffusive processes (sheet and splash erosion). This result is consistent with the current soil erosion theory which suggests a dependence of sheet and splash erosion processes on rainfall intensity. Likewise, when relating surface change metrics to runoff rate, R^2 was improved by excluding diffusive processes which is consistent with a dependence of concentrated flow processes (channel geometry) on runoff discharge.

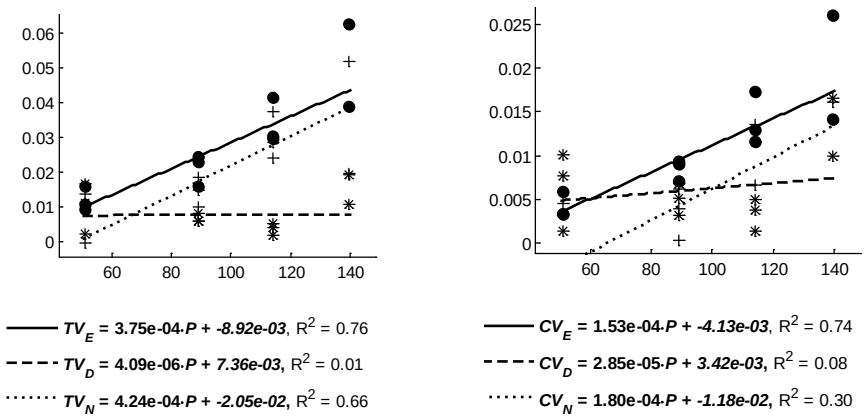

Figure 5 Plot-wide and channel erosion and deposition volumes as a function of precipitation

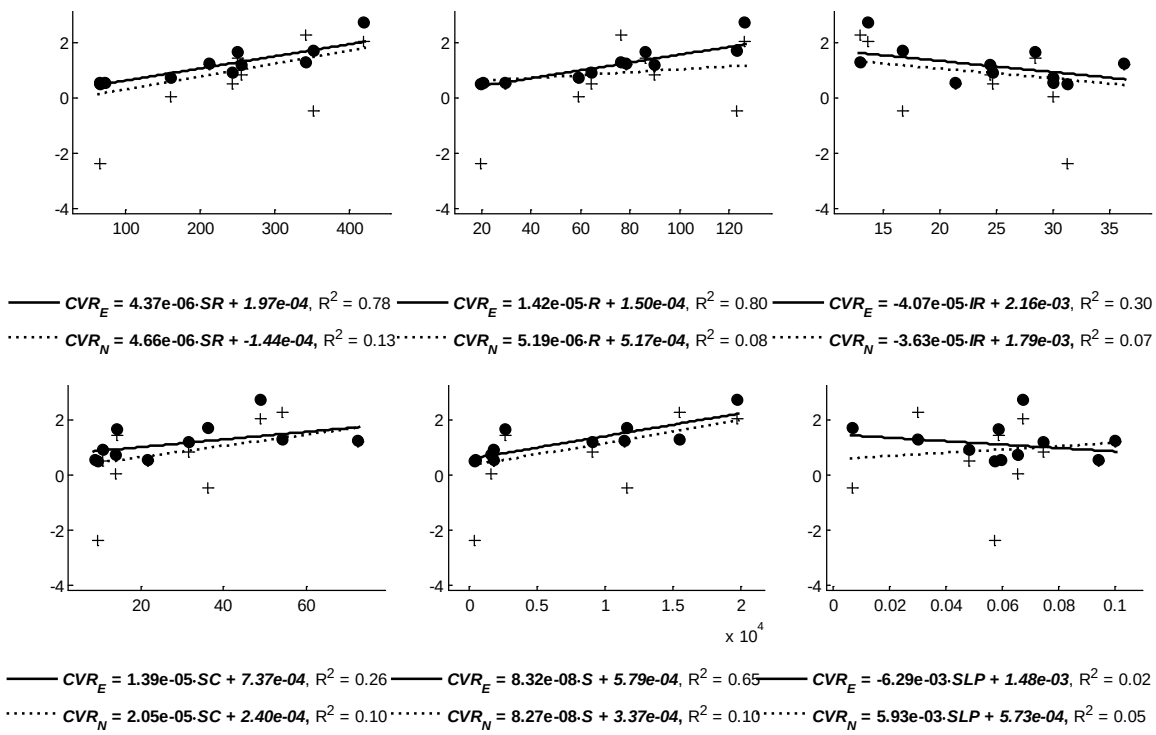

Figure 6 Area and volume-based ratios of flow concentration as a function hydrology, soil loss and slope

The ratios of flow concentration determined using volumes are shown in Figure 6. Overall the volume-based ratios showed again a stronger correlation with explanatory variables than the area-based ones. Also, an improvement in R^2 was observed with CVR_E compared to CV_E in Figure 4. This might be explained by the fact that CVR_E normalized channel erosion volumes to plot size and non-erodible contents (vegetation) which varied between plots due to practical field constraints. The R^2 values associated with CVR_N were, however, degraded compared to CV_N which is likely the result of confounding factors of deposition processes.

Figure 7 shows the relationship between α and α' (related to the energy spent on channel network expansion) as a function of hydrology and slope. A key finding that emerges from this analysis is that the hydrologic variable correlated better with α' than it did with α, suggesting that even though deposition volume might not be directly controlled by hydrologic parameters (Figure 3 and 4), its consideration is

essential in quantifying energy dissipated on channel widening. In other words, there might be a limit to sediment transport off-site for every incremental increase in runoff discharge (transport capacity concept).

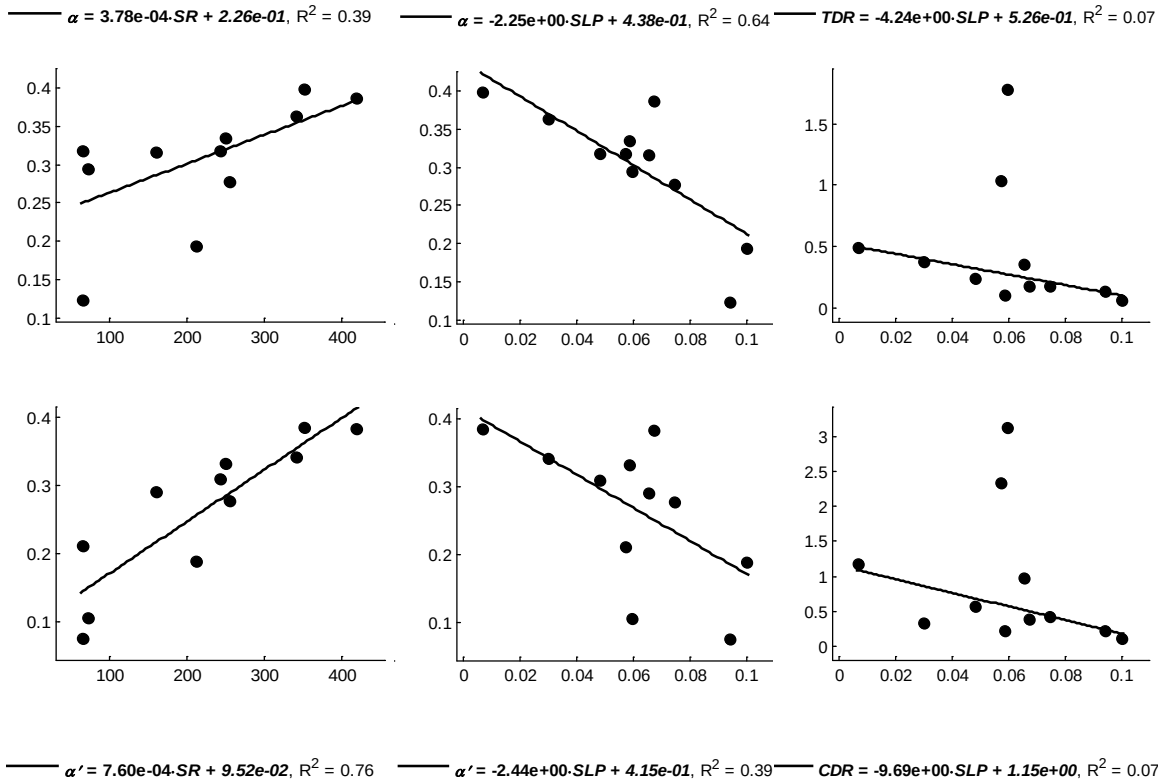

Figure 7 Volume-based channel expansion ratios (α = erosion volume based and α' = net volume based) as a function hydrology (*SR*) and slope. And plot-wide (*TDR*) and channel (*CDR*) deposition ratios as a function of slope

Another key finding in Figure 7 is the negative and relatively strong (R^2 = 0.64 for α and 0.39 for α') relationship between lateral energy expenditure and slope, consistent with the process of increase in downcutting relative to lateral expansion as slope increases. Also, Figure 7 shows that slope is negatively related to the proportion of re-deposited material (*TDR* and *CDR*), but the low number of observations adversely impacted the resulting R^2.

CONCLUSIONS

Rainfall simulations were conducted in saline rangeland communities of the Upper Colorado River Basin to quantify rainfall-driven salt transport from these environment to surface waters. Hydrology, erosion and high-resolution changes in surface microtopography measured during these simulations, were used in this study to answer many questions relevant to sediment transport processes in these saline rangelands and other sparsely vegetated rangelands.

Preliminary data show that analysis of the high resolution DEMs revealed that many interesting sediment transport processes that are traditionally difficult to quantify can now be examined with details and related to hydrologic inputs and landscape properties. Some of the key preliminary findings supported by our data include:

(1) the dependence of deposition on plot slope and its independence on hydrologic and soil loss variables,
(2) data supporting the process of increased downcutting as slope increased,
(3) significance of accounting deposition processes in overall runoff energy quantification,
(4) evidence of the existence of an equilibrium channel geometry with a given discharge that is marginally impacted by runoff duration.

This study will be valuable in developing semi-empirical equations for spatial extent and mass partitioning of soil loss between diffusive processes and concentrated flow erosion, as well as providing much needed insight into the processes of deposition and sediment storage.

REFERENCES

Agisoft LLC. (2013). Agisoft photoscan professional edition. Agisoft LLC, Russia.

Al-Hamdan O.Z., Pierson F.B., Nearing M.A., Williams C.J., Stone J.J., Kormos P.R., Boll J., Weltz M.A. (2012). Concentrated flow erodibility for physically based erosion models: Temporal variability in disturbed and undisturbed rangelands. Water Resources Research 48. doi:10.1029/2011wr011464.

Bagnold R.A. (1977). Bed load transport by natural rivers. Water Resources Research 13: 303-312. doi:10.1029/WR013i002p00303.

Bagnold R.A. (1980). An empirical correlation of bedload transport rates in flumes and natural rivers. Proceedings of the Royal Society of London Series a-Mathematical Physical and Engineering Sciences 372: 453-473. doi:10.1098/rspa.1980.0122.

ASCE. (1980). Universal soil loss equation and rangelands. Symposium on Watershed Management, Boise, ID. ASCE.

Bowles D.S., Nezafati H., Bhasker R.K., Riley J.P., Wagenet R.J. (1982). Salt loading from efflorescence and suspended sediments in the price river basin. Water Resources Planning Series. Utah Water Research Laboratory, Utah State University, Logan, Utah. p. 142.

ESRI. (2011). Arcgis desktop release 10. Evironmental Systems Research Institute, Redlands, CA.

Foster G.R., Simanton J.R., Renard K.G., Lane L.J., Osborn H.B. (1981). Application of the universal soil loss equation to rangelands on a per-storm basis - discussion. Journal of Range Management 34: 161-165. doi:10.2307/3898140.

General Public Licence. (2014). Cloudcompare v2.5. General Public Licence, USA.

Ghebreiyessus Y.T., Gantzer C.J., Alberts E.E. (1994). Soil erosion by concentrated flow: Shear stress and bulk density. Transactions of the ASAE 37: 1791-1797.

Hart G.E. (1984). Erosion from simulated rainfall on mountain rangeland in utah. Journal of Soil and Water Conservation 39: 330-334.

Hawkins R.H., Gifford G.F., Jurinak J.J. (1977). Effects of land processes on the salinity of the upper colorado river basin: Final project report. Utah State University, Logan, Utah. p. 196.

(2006). Extraction of stream channels in high-resolution digital terrain images using morphology. Geoscience and Remote Sensing Symposium, 2006. IGARSS 2006. IEEE International Conference on, July 31 2006-Aug. 4 2006.

Johnson C.W., Savabi M.R., Loomis S.A. (1984). Rangeland erosion measurements for the usle. Transactions of the ASAE 27: 1313-1320.

Laflen J.M., Lane L.J., Foster G.R. (1991). Wepp - a new generation of erosion prediction technology. Journal of Soil and Water Conservation 46: 34-38.

Lyle W., Smerdon E. (1965). Relation of compaction and other soil properties to erosion resistance of soils. Trans. ASAE 8: 419-422.

Mitchell J.E., Roundtable S.R. (2010). Criteria and indicators of sustainable rangeland management. University of Wyoming, Cooperative Extension Service.

Nearing M., Norton L., Bulgakov D., Larionov G., West L., Dontsova K. (1997). Hydraulics and erosion in eroding rills. Water Resources Research 33: 865-876.

Nearing M.A., Wei H., Stone J.J., Pierson F.B., Spaeth K.E., Weltz M.A., Flanagan D.C., Hernandez M. (2011). A rangeland hydrology and erosion model. Transactions of the Asabe 54: 901-908.

Nichols M.H., Nearing M.A., Polyakov V.O., Stone J.J. (2013). A sediment budget for a small semiarid watershed in southeastern arizona, USA. Geomorphology 180: 137-145. doi:10.1016/j.geomorph.2012.10.002.

Paige G.B., Stone J.J., Smith J.R., Kennedy J.R. (2004). The walnut gulch rainfall simulator: A computer-controlled variable intensity rainfall simulator. Applied Engineering in Agriculture 20: 25-31.

Pierson F.B., Williams C.J., Hardegree S.P., Clark P.E., Kormos P.R., Al-Hamdan O.Z. (2013). Hydrologic and erosion responses of sagebrush steppe following juniper encroachment, wildfire, and tree cutting. Rangeland Ecology & Management 66: 274-289. doi:10.2111/rem-d-12-00104.1.

Riley J.P., Bowles D.S., Chadwick D.G., Grenney W.J. (1979). Preliminary identification of price river basin salt pickup and transport processes. JAWRA Journal of the American Water Resources Association 15: 984-995. doi:10.1111/j.1752-1688.1979.tb01077.x.

Riley J.P., Chadwick D.G., Dixon L.S., James L.D., Grenney W.J. (1982). Salt uptake in natural channels traversing mancos shales in the price river basin , utah.

Rodriguez F., Maire E., Courjault-Radé P., Darrozes J. (2002). The black top hat function applied to a dem: A tool to estimate recent incision in a mountainous watershed (estibère watershed, central pyrenees). Geophysical Research Letters 29: 9-1-9-4. doi:10.1029/2001GL014412.

Schwanghart W., Groom G., Kuhn N.J., Heckrath G. (2013). Flow network derivation from a high resolution dem in a low relief, agrarian landscape. Earth Surface Processes and Landforms 38: 1576-1586. doi:10.1002/esp.3452.

Spaeth K.E., Pierson F.B., Weltz M.A., Blackburn W.H. (2003). Evaluation of usle and rusle estimated soil loss on rangeland. Journal of Range Management 56: 234-246. doi:10.2307/4003812.

Torri D., Sfalanga M., Chisci G. (1987). Threshold conditions for incipient rilling. Catena: 97-105.

Trieste D.J., Gifford G.F. (1980). Application of the universal soil loss equation to rangelands on a per-storm basis. Journal of Range Management 33: 66-70. doi:10.2307/3898231.

Tuttle M.L., Grauch R.I. (2009). Salinization of the upper colorado river—fingerprinting geologic salt sources. USGS Scientific Investigations Report. U.S. Geological Survey, Reston, Virginia. p. 62.

Weltz M.A., Kidwell M.R., Fox H.D. (1998). Invited synthesis paper: Influence of abiotic and biotic factors in measuring and modeling soil erosion on rangelands: State of knowledge. Journal of Range Management 51: 482-495. doi:10.2307/4003363.

Wirtz S., Seeger M., Zell A., Wagner C., Wagner J.F., Ries J.B. (2013). Applicability of different hydraulic parameters to describe soil detachment in eroding rills. Plos One 8. doi:10.1371/journal.pone.0064861.

Zhang G.H., Liu B.Y., Liu G.B., He X.W., Nearing M.A. (2003). Detachment of undisturbed soil by shallow flow. Soil Science Society of America Journal 67: 713-719.

Disclaimer: The use of trade, firm, or corporation names in these methods is for the information and convenience of the reader. Such use does not constitute an official endorsement or approval by the Federal Government, of any product or service to the exclusion of others that may be suitable.